Writhe formulas and antipodal points in plectonemic DNA configurations

Sébastien Neukirch

Institut Jean le Rond d'Alembert, CNRS and UPMC Univ. Paris 6, 4 Place Jussieu (case 162), 75005 Paris, France

Eugene L. Starostin

*Centre for Nonlinear Dynamics, Department of Civil, Environmental and Geomatic Engineering, University College London,
London, United Kingdom*

The linking and writhing numbers are key quantities when characterizing the structure of a piece of super-coiled DNA. Defined as double integrals over the shape of the double helix, these numbers are not always straightforward to compute, though a simplified formula was established in a theorem by Fuller [Proc. Natl. Acad. Sci. U.S.A. **75**, 3557 (1978)]. We examine the range of applicability of this widely used simplified formula, and show that it cannot be employed for plectonemic DNA. We show that inapplicability is due to a hypothesis of Fuller theorem that is not met. The hypothesis seems to have been overlooked in many works.

PACS number(s): 87.10.−e, 87.14.gk, 02.40.−k, 87.15.−v

I. INTRODUCTION

The double-helix structure of DNA is the source of many complications in its *in-vivo* functioning during condensation-decondensation, replication, or transcription. For example, the necessary unzipping of the molecule during transcription induces torsional strain along DNA. The development of magnetic tweezers [1,2] or the use of quartz cylinders in optical tweezers [3] allow researchers to investigate the *in-vitro* response of DNA molecules to torsional stress. Studies of the behavior of this twist storing polymer are not just a game for physicists as it has been clearly established that, e.g., the assembly of RecA could be stalled by torsional constraints [4], or that the rate of formation and the stability of the complex formed by promoter DNA and RNA polymerase depends on the torque present in the DNA molecule [5]. On the theoretical side, matters are made difficult by the nonlocality of the topological property that is associated with the torsional constraint: The link. The two sugar-phosphate backbones of DNA have opposite orientation and the ends of a double-stranded DNA molecule can only be chemically bound in such a way that each strand joins itself, thereby yielding two interwound closed curves (no Möbius-like configuration can exist). For a circularly closed DNA molecule, the link is the number of times one of the sugar-phosphate backbone winds around the other. Once the three-dimensional shape of the molecule is projected onto a plane, the link is given by one-half the number of signed crossings between the two backbones. This quantity is best seen as the number of turns put in an initially planar plasmid (a piece of circularly closed double-stranded DNA) before closing it. The link has been shown to consist of two parts: The two sugar-phosphate backbones of a plasmid can be linked because (i) the plasmid lies in a plane but the base pairs are twisted around their center line (the curve joining the centroids of the base pairs) and/or (ii) the center line itself follows a writhed path in space. In general the two possibilities coexist and the link Lk of a DNA molecule is the addition of the two quantities [6–9],

$$Lk = Tw + Wr. \tag{1}$$

The twist Tw is a local quantity in the sense that it can be computed as the single integral of the twist rate $\tau(s)$: $2\pi Tw = \int_0^L \tau(s) ds$, where s is the arclength along the center line and L is the total contour length of the molecule. In elastic DNA models, the twist rate $\tau(s)$ is normally coupled to mechanical quantities (e.g., the torque) characterizing the molecule. Contrary to the twist, Wr is a global property of the center line of the molecule. We first define the directional writhe of a closed curve Γ. Consider a closed curve in three dimensions (3D) and project this curve, along a certain direction, on a plane. The number of signed crossings seen in the plane is the directional writhe for that direction. One could then reiterate the procedure with different directions of projection and compute the directional writhe for each direction. The average value obtained for the directional writhes, when all directions are considered, is the writhe $Wr(\Gamma)$ of the 3D curve Γ [10].

II. GLOBAL AND LOCAL WRITHE FORMULAS

The following double integral has been introduced by Călugăreanu [6,7] and White [8],

$$Wr^{CW}(\Gamma) = \frac{1}{4\pi} \int_\Gamma \int_\Gamma \frac{[t(s) \times t(s')] \cdot [r(s) - r(s')]}{|r(s) - r(s')|^3} ds ds', \tag{2}$$

where $r(s)$ is the position of points on Γ and $t(s)$ is the unit tangent to Γ. As soon as a 3D curve does not self-intersect, the writhe $Wr(\Gamma)$ of the curve is given by Eq. (2): $Wr(\Gamma) = Wr^{CW}(\Gamma)$ if $r(s) \neq r(s') \forall s, s'$ with $s \neq s'$.[1] The computation of the double integral of Eq. (2) is analytically hard and numerically time consuming to perform. An important result though enables one to reduce the double integral to a single

---

[1]The double integral may be shown to converge for self-crossing curves provided the tangents at the intersection points are not aligned [11].

integral, provided several hypotheses are fulfilled [12]. It is the main purpose of this paper to show that these hypotheses are not met in the case of plectonemic DNA.

Fuller's theorem [12] states that the writhe of the curve Γ can be computed by considering the writhe of a reference curve Γ_0 (which should be known or easy to compute) and the continuous deformation (a homotopy) morphing Γ_0 to Γ,

$$Wr(\Gamma) \overset{?}{=} Wr^F(\Gamma, \Gamma_0) \overset{\text{def}}{=} Wr(\Gamma_0) + \frac{1}{2\pi} Fu(\Gamma, \Gamma_0), \qquad (3)$$

where

$$Fu(\Gamma, \Gamma_0) = \int_0^{\sigma_L} \frac{t_0(\sigma) \times t(\sigma)}{1 + t_0(\sigma) \cdot t(\sigma)} \cdot \frac{d}{d\sigma}[t_0(\sigma) + t(\sigma)] d\sigma,$$

where $t_0(\sigma) \overset{\text{def}}{=} [dr_0(\sigma)/d\sigma]/|dr_0(\sigma)/d\sigma|$ is the unit tangent to Γ_0 and where $\sigma \in [0, \sigma_L]$ is a common parametrization for both curves, though not necessarily the arclength along Γ or Γ_0. The total contour length of Γ is L. The curve Γ_0 is normally chosen to be a fairly simple curve (e.g., planar with zero writhe) so the computation of $Wr(\Gamma)$ boils down to estimating the single integral in Eq. (3). Before doing so, one should verify whether the hypotheses of Fuller's theorem are fulfilled [this is the sense of the question mark in Eq. (3)]. The continuous deformation from Γ_0 to Γ introduces a family of curves Γ_λ with $\lambda \in [0, 1]$ and $\Gamma_1 \equiv \Gamma$. The unit tangent to Γ_λ is

$$t_\lambda(\sigma) \overset{\text{def}}{=} [dr_\lambda(\sigma)/d\sigma]/|dr_\lambda(\sigma)/d\sigma|.$$

The first hypothesis is that none of the curves Γ_λ self-intersects. The second hypothesis is that, and this is the point we want to emphasize, there should be no point along any of the curves Γ_λ where $t_\lambda(\sigma) \cdot t_0(\sigma) = -1$. For each value of λ, the (unit) tangent $t_\lambda(\sigma)$ with $\sigma \in [0, \sigma_L]$ defines a curve, called the tangent indicatrix, on the unit sphere. If for a certain $\bar{\lambda}$ and a certain $\bar{\sigma}$ we have $t_{\bar{\lambda}}(\bar{\sigma}) \cdot t_0(\bar{\sigma}) = -1$ then, on the unit sphere, the point corresponding to $t_{\bar{\lambda}}(\bar{\sigma})$ is antipodal to the point corresponding to $t_0(\bar{\sigma})$. For brevity we shall also call antipodal the point $r_{\bar{\lambda}}^-(\bar{\sigma})$ or the curve $\Gamma_{\bar{\lambda}}^-$ itself.

In models where self-intersection is prevented (e.g., models using hard- or soft-wall potentials of the molecule on itself) a continuous deformation free of self-intersection (an isotopy) may be easy to devise and the first hypothesis would be verified. However nothing in these models ensure that the second hypothesis (that no antipodal points exist for all $\lambda \in [0, 1]$ and all $\sigma \in [0, \sigma_L]$) is met and consequently Fuller's formula (3) cannot be used to compute the writhe. We nevertheless remark that even in the case of self-intersection or antipodal points Fuller's formula is always correct *modulo* 2: The integer, and most important, part of $Wr(\Gamma)$ will not be correct, but the fractional part will. Each antipodal point present in the continuous deformation from Γ_0 to Γ introduces a shift of two units between the actual writhe $Wr(\Gamma)$ of the curve Γ and the value $Wr^F(\Gamma, \Gamma_0)$ [13]. Consequently, if there are m antipodal points along the deformation $\lambda \in [0, 1]$, the computed value Wr^F could be as far as $2m$ from the correct value Wr, but the fractional part will be accurate.
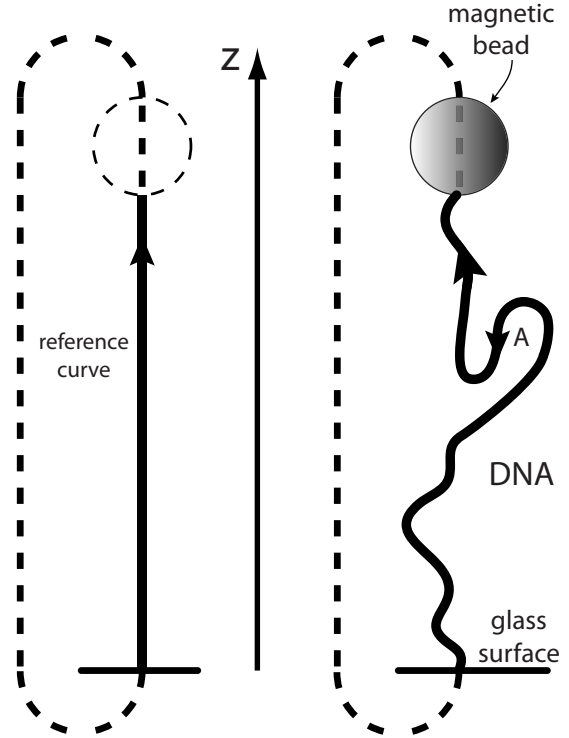

FIG. 1. The shape of a DNA molecule subjected to a vertical pulling force follows a 3D curve which is locally made random by thermal agitation. As explained in [14], when the force is small or moderate, points where the tangent to the molecule is oriented downward can appear, e.g., point A. These points on the curve are antipodal to corresponding points on the reference curve.

This discrepancy between Wr^F and the actual writhe Wr has already been pinpointed in the case where DNA is treated as a fluctuating chain under low twist (i.e., without plectonemes) [14–16]. Nevertheless we have found a certain number of references where Fuller's formula is used [17–34]. In most cases the hypotheses of Fuller's theorem were not checked, if only mentioned. In some works the formula is used in a scheme that provides an estimate for the torsional stiffness of the DNA molecule [20,21] and this has been shown to lead to incorrect results [35,15,14]. Nevertheless, in some papers [34,19,22,23], the formula was used to assess the writhe of DNA configurations under high stretching force and low twist, in which cases antipodal points are absent and the formula is correct.

III. WRITHE AND LINK OF DNA MOLECULES IN MAGNETIC TWEEZER EXPERIMENTS

During a force-extension experiment on a single DNA molecule thermal agitation deforms the molecule whose shape locally adopts random directions (Fig. 1, left-hand side). In the absence of (or under low) twist, DNA is modeled as a wormlike chain [36]; the path followed by its center line in space looks like a (directed) random walk [19]. In such configurations, the writhe is usually evaluated using Fuller's formula (3) with the reference curve shown in Fig. 1, left-hand side. Since the writhe is classically defined for a

closed curve, the reference and actual curves are all closed by imaginary C-shaped curves (dashed in Fig. 1) that connect the top to the base of the configurations. (Other choices of closures and interferences due to the closure in the computation of the writhe are discussed in [14,11,37,38,16].) Strictly speaking the curve Γ for which we compute the writhe consists of two parts: The closure and the part corresponding to the molecule. As the closure remains unchanged in the continuous deformation $\lambda \in [0,1]$ its contribution to Fuller's integral is zero. Consequently, we will forget about the closure and call Γ the (open) curve described by the molecule only. The reference curve Γ_0 is then the z axis, and Fuller's formula (3) becomes

$$Wr^F(\Gamma,\Gamma_0) = Wr(\Gamma_0) + \frac{1}{2\pi}\int_0^L \frac{\boldsymbol{e}_z \times \boldsymbol{t}(s)}{1+\boldsymbol{e}_z \cdot \boldsymbol{t}(s)} \cdot \frac{d}{ds}\boldsymbol{t}(s)ds$$

$$= 0 + \frac{1}{2\pi}\int_0^L [1-\cos\,\theta(s)]\frac{d\psi(s)}{ds}ds, \qquad (4)$$

if the tangent $\boldsymbol{t}(s) = (\sin\theta\cos\psi, \sin\theta\sin\psi, \cos\theta)$ is parametrized by Euler angles $\theta(s) \in [0,\pi]$, and $\psi(s) \in [0,2\pi)$. As stated above, Eq. (4) is only valid if the curve Γ can be deformed into the reference curve Γ_0 without passing through configurations Γ_λ having their tangent vector $\boldsymbol{t}_\lambda(\sigma)$ facing $-\boldsymbol{e}_z$: $\boldsymbol{t}_\lambda(\sigma) \neq -\boldsymbol{e}_z$ for all λ, σ. We remark that in the present case where Γ_0 is the z axis an antipodal point is a point where the curve $\boldsymbol{t}_\lambda(\sigma)$ passes through the south pole of the unit sphere $\theta(\sigma) = \pi$.

In the case where the actual configuration Γ exhibits a single or multiple antipodal points it has been proposed in [21] to evaluate the writhe from Eq. (4) with Euler angles defined on a truncated unit sphere: θ would not be allowed to reach π and hence antipodal points would be avoided (the curve $\widetilde{\Gamma}$ so defined would be very near the real curve Γ, hence the writhes would almost be the same). We stress that this process is not sufficient as even for a given curve with no antipodal points, it is not clear whether Eq. (4) is valid or not. In order for Eq. (4) to be valid, one must exhibit a continuous deformation from the z axis to the curve Γ that is entirely free of antipodal points. There are many cases where the actual curve Γ is free of antipodal points, but where a deformation free of antipodal points does not exist. Consequently in these cases Eq. (4) yields an incorrect result (unless antipodal points of opposite signs cancel out). Nevertheless, it has been noted that under high stretching force (e.g., $F \sim 5$ pN) and low torque the DNA molecule is almost straight and no such antipodal points exist [23]. In such a case Fuller's formula is correct provided no plectonemes are present, as we will see now.

In magnetic tweezer experiments, when a large amount of turns are put in (by rotation of the magnetic bead around the z axis), the DNA molecule reacts by forming plectonemes [40]. The number of turns n imposed on the magnetic bead is given by the link Lk of the molecule. We now show that the presence of plectonemes in the supercoiled configuration prevents the existence of a deformation, from Γ_0 (i.e., the z axis) to Γ, that is free of antipodal points, and consequently forbid the use of Eq. (4).

In terms of the Euler angles the twist of the molecule can be computed as

$$Tw = \frac{1}{2\pi}\int_0^L \left(\frac{d\phi}{ds} + \cos\,\theta\frac{d\psi}{ds}\right)ds, \qquad (5)$$

where $\phi(s)$ is the third Euler angle (see, e.g., [41]). Using Eqs. (4) and (5) we obtain

$$Lk^F = \frac{1}{2\pi}\int_0^L \frac{d}{ds}(\phi+\psi)ds. \qquad (6)$$

This formula usually is the starting point for computations of the link of supercoiled configurations, see, e.g., [21] or [17]. We show here that it yields incorrect results when plectonemes are present. We have performed computations to model the elastic response of a twist storing filament subject to tensile and torsional constraints and we quantitatively reproduced the plectonemic regime characterized by the linear decrease of the end-to-end distance of the filament as a function of the number n of turns put in [39]. The plectonemic configurations were computed numerically using a continuation algorithm and $n = Lk$ was computed by continuity so that no integer number of turns is missed [we also performed numeric integration of the double integral of Eq. (2) for the writhe of the configurations, with closures, and always obtained consistent results]. These shapes serve as an illustration for the computation of the writhe and consequently are used for their geometry only. The fact that they are mechanical equilibria is not relevant here. The continuous dark curve in Fig. 4 shows an output of the numerics, drawn in the (Lk,Z) plane, where Z is the vertical extension of the molecule. The curve starts at point O which corresponds to a straight and twisted configuration. The path is then monotonically decreasing in Z. We have selected five configurations A, B, C, D, and E which are drawn in Fig. 2, together with their corresponding tangent indicatrices (see definition in Sec. II) drawn in Fig. 3. Configurations B and D each comprise an antipodal point located at the middle point of the end loop of the plectonemic structure. This can be verified in Fig. 3 B and D, where the tangent indicatrices pass through the south pole of the unit sphere.

Using the same geometric configurations, we compute Lk^F from Eq. (6) and we plot the corresponding curve, in gray, on the same diagram. We see that each antipodal event introduces a shift of two units in the gray curve, which is consequently broken. As expected this confirms that Eq. (6) is only valid modulo 2 and hence should not be used to estimate the link of plectonemic configurations. The writhe and link of the five configurations are given in Table I where they are compared with Wr^F and Lk^F given by Eqs. (4) and (6). For configuration E, which is separated from the reference curve by two antipodal events, we see that Wr^F (respectively, Lk^F) is four units away from the correct Wr (respectively, Lk) value. This configuration E is an illustration of the fact that Fuller's formulas [Eq. (4) or (6)] can be wrong even for a configuration that does not comprise any antipodal point, which is clearly illustrated in E of Fig. 3 where we see that the tangent indicatrix is nowhere near the south pole.
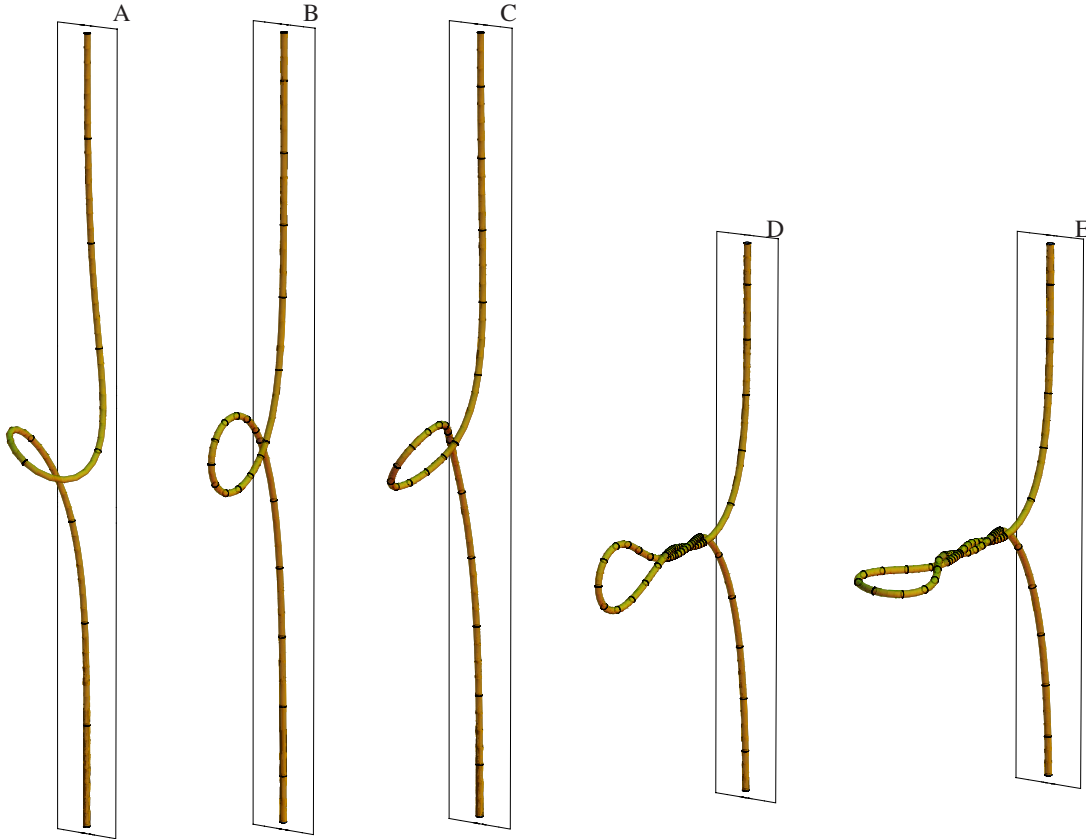
FIG. 2. (Color online) Configurations *A*, *B*, *C*, *D*, and *E* (see Fig. 4) obtained by numerical continuation [39]. Configurations *B* and *D* each have an antipodal point to the reference curve of Fig. 1. These antipodal points are located at the middle point of the end loop of the plectonemic structure.

We first comment on the size of the gap between the two curves. A plectonemic DNA configuration Γ that shows N_x (positive) crossings on a lateral projection has $Wr(\Gamma) \simeq +N_x$ [42]. If we continuously deform this configuration to the reference curve Γ_0 of Fig. 1, left-hand side, by unwinding the plectonemic region, an antipodal point arises each time the tangent at the apex of the terminal loop (at the end of the plectonemic region) is facing downward. This happens $N_x/2$ times. As proved in [13] the presence of $m = N_x/2$ antipodal points leads to a discrepancy in Fuller's formula of $2m$, $|Wr - Wr^F| \leq 2m$. Since $2m = N_x \simeq Wr$, we have that $0 \lesssim Wr^F \lesssim 2Wr$, which corresponds to an error of up to 100%. This is apparent in Fig. 4 where the broken gray curve stays near the

TABLE I. Writhe (first line) and link (third line) of the configurations of Fig. 2, computed by continuation or use of the double integral [Eq. (2)]. The second line is computed from Eq. (4) and the last line is computed from Eq. (6). Formulas (4) and (6) are not applicable on configurations *B* and *D* that each have an antipodal point, and yield incorrect results for configurations *C* and *E*.

	A	B	C	D	E
Wr	0.70	0.99	1.09	2.92	3.45
Wr^F	0.70		−0.91		−0.55
Lk	4.46	1.84	4.15	4.23	4.75
Lk^F	4.46		2.15		0.75

vertical axis while the (continuous) dark curve monotonically increases in the link.

Second we note that the discrepancy between the two curves occurs shortly after self-contact has started in the filament, for $n \simeq 1$, see inset of Fig. 4. Plectonemic structure may exist for a small number of turns n, provided the pulling force is not too large. On the other hand, a large pulling force does not rule out the occurrence of plectonemes, provided that n is large enough. This leaves a small parameter regime (large pulling force, low number of turns) where plectonemes are absent. When the two sources of discrepancies are considered (random walk antipodal points [14,15], and plectonemic antipodal points) one sees that the use of Eq. (4) [respectively, Eq. (6)] to compute the writhe (respectively, the link) in a model for DNA under tensile and/or torsional stress is to be avoided unless $n \simeq 0$ and the tensile force is large.

IV. DISCUSSION AND CONCLUDING REMARKS

We summarize here few properties of the quantities $Wr^{CW}(\Gamma)$, $Wr^F(\Gamma, \Gamma_0)$ which do not always give the writhe of a curve Γ. The quantity $Wr^{CW}(\Gamma)$ is a function of the curve Γ only, whereas the quantity $Wr^F(\Gamma, \Gamma_0)$ also depends on the reference curve Γ_0. The quantity Wr^{CW} yields the correct value for the writhe Wr of a closed curve as soon as the curve is not self-intersecting. Along a continuous deforma-
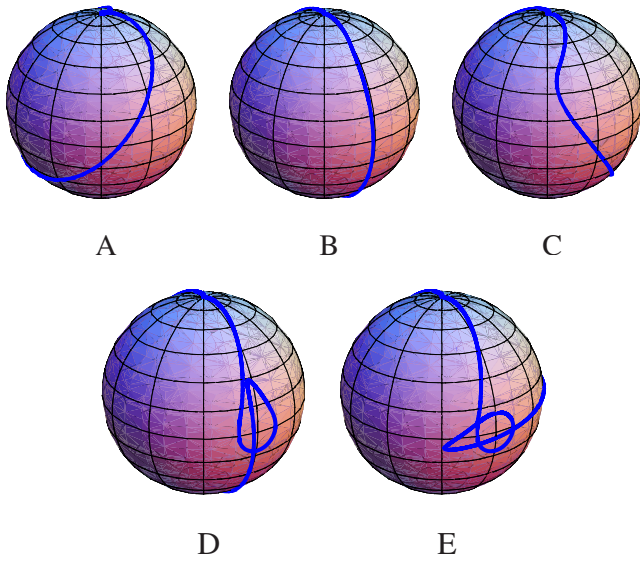
FIG. 3. (Color online) Tangent indicatrices of configurations *A*, *B*, *C*, *D*, and *E* of Fig. 2. An antipodal point arises when the curve passes through the south pole of the sphere, i.e., for configurations *B* and *D*.
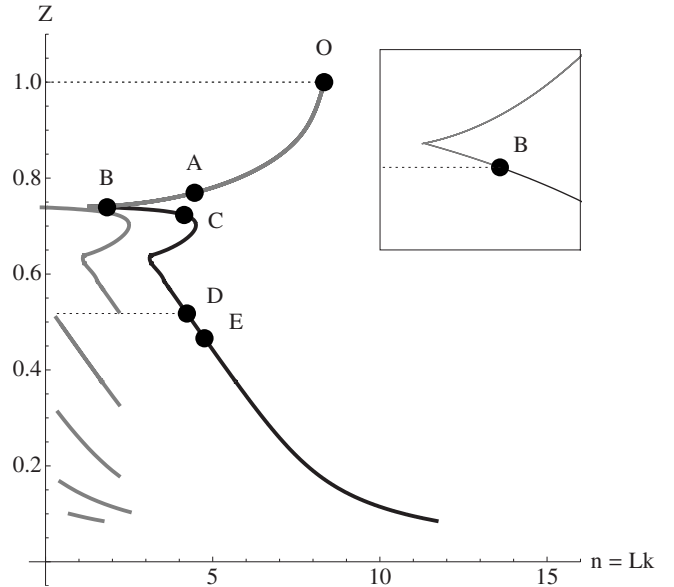

FIG. 4. The dark continuous curve is obtained from numerical continuation [39] and the broken gray curve is obtained from Eq. (6). Five configurations *A*, *B*, *C*, *D*, and *E* are selected and plotted in Fig. 2 together with their tangent indicatrices in Fig. 3. The inset shows a zoom around point *B*, the first antipodal point, where the gray curve jumps by an amount of −2 units. From *O* to *B* the two curves coincide.

tion Γ_λ with $\lambda \in [0,1]$ (with $\Gamma_1 \equiv \Gamma$), the quantity $Wr^{CW}(\Gamma_\lambda)$ jumps by two units when the curve Γ_λ intersects itself (say at $\lambda = 1/2$). Since the writhe Wr also jumps by two units, the quantity Wr^{CW} is equal to Wr before and after the self-crossing event, i.e., $Wr^{CW}(\Gamma_\lambda) = Wr(\Gamma_\lambda)$, $\forall \lambda \neq 1/2$. Now the quantity Wr^F has no such discontinuity: Along a continuous deformation where the curve self-intersects, the writhe Wr will jump by two units, but the quantity Wr^F will stay continuous. This means that the quantity Wr^F no longer yields the correct value for the writhe after the self-crossing event, $Wr^F(\Gamma_\lambda, \Gamma_0) = Wr(\Gamma_\lambda)$, $\forall \lambda < 1/2$ but $Wr^F(\Gamma_\lambda, \Gamma_0) \neq Wr(\Gamma_\lambda)$, $\forall \lambda > 1/2$. The same is true for antipodal points. Along a continuous deformation Γ_λ with $\lambda \in [0,1]$, the quantity $Wr^F(\Gamma_\lambda, \Gamma_0)$ jumps by two units when the curve Γ_λ has an antipodal point (say at $\lambda = 1/2$) with regard to the reference curve Γ_0. On the other hand, the writhe Wr stays continuous. This means that the quantity Wr^F no longer yields the correct value for the writhe as soon as an antipodal event happens, $Wr^F(\Gamma_\lambda, \Gamma_0) = Wr(\Gamma_\lambda)$, $\forall \lambda < 1/2$ but $Wr^F(\Gamma_\lambda, \Gamma_0) \neq Wr(\Gamma_\lambda)$, $\forall \lambda > 1/2$. This is an important point and many authors seem to believe that the quantity $Wr^F(\Gamma_\lambda, \Gamma_0)$ only has problems for configurations actually comprising an antipodal point ($\lambda = 1/2$ in the above example). Therefore, the quantity $Wr^F(\Gamma, \Gamma_0)$ may not be equal to the writhe $Wr(\Gamma)$ even for curves that do not comprise any antipodal point. This makes use of $Wr^F(\Gamma, \Gamma_0)$ uneasy, as one must first verify the absence of antipodal events in the entire continuous deformation $\Gamma_0 \rightarrow \Gamma$. On the contrary the use of $Wr^{CW}(\Gamma)$ is much easier in the sense that one must only check that the actual curve Γ does not self-intersect. In this sense the quantities $Wr^{CW}(\Gamma)$ and $Wr^F(\Gamma, \Gamma_0)$ do not suffer from the same pathologies in the computation of the writhe, contrarily to what is claimed in [43]. Another consequence is that, when sampling DNA configurations to construct a statistical ensemble and compute writhe averages and fluctuations, it is not enough to introduce, as was done in [21], a small forbidden

region around the south pole of the unit sphere to ensure that $Wr^F(\Gamma, \Gamma_0)$ yields a correct value. In fact many of these sampled configurations, even free of antipodal points, are configurations that suffer the same problems as the configurations with $\lambda > 1/2$ above: $Wr^F(\Gamma, \Gamma_0) \neq Wr(\Gamma)$, as numerically verified in [14,15].

Finally we want to point out the following property. We saw that if a continuous deformation Γ_λ with $\lambda \in [0,1]$ contains an antipodal event, then $Wr^F(\Gamma, \Gamma_0)$ does not yield the correct result after the antipodal event. Now one can argue that yet another continuous deformation, free of antipodal events and self-crossings, may exist (with the same initial and final curves) and that in this case $Wr^F(\Gamma, \Gamma_0)$ would yield the correct result. This is not the case since, as we show in Appendix B, as soon as a corrupted deformation exists in between two curves Γ_0 and Γ, then all continuous deformations are corrupted and $Wr^F(\Gamma, \Gamma_0)$ definitely yields an incorrect result. This means that the reference curve Γ_0 cannot be used. One is bound to find another reference curve or to use the double integral Wr^{CW}. It appears that an easy way to verify the applicability of Fuller formula (3) between an actual curve and a reference curve is to consider any convenient deformation that avoids antipodal events. This can always be done if one allows for self-crossings. Then formula (3) is applicable if and only if the net sum of self-crossings is zero.

In the case of numerical computations, either dealing with continuation of mechanical equilibria or statistical ensembles of configurations, the writhe can be assessed in an accurate way by using both the double integral (2) and Fuller integral (4) in a cooperative way. The double integral being time consuming to evaluate, one can in a first step discretize it
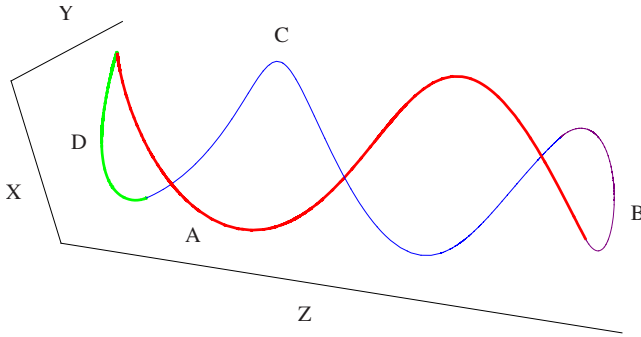
FIG. 5. (Color online) Circularly closed supercoiled plasmid corresponding to curve $\Gamma = \Gamma_A \cup \Gamma_B \cup \Gamma_C \cup \Gamma_D$ with $\theta_A = \pi/6$ and $L_A = 5\pi$.

[44] with a reduced number of elements so that it produces an approximate result that only must be accurate up to ± 1 (one still must estimate how many elements are needed to obtain such an accuracy [45]). Then in a second step, Fuller integral is used to refine the result. Even if Fuller integral may be off by several integers, its fractional part is correct. In this scheme, the double integral yields the integer part of the writhe and Fuller integral yields the fractional part of the writhe. Moreover, in cases where one knows the correct value of the writhe of a nearby configuration (e.g., a predecessor configuration, one move away in a Monte Carlo scheme) this value can be used as the approximate result of the first step and one only must compute Fuller integral to obtain a correct and accurate value of the writhe. (The usual assumption that there is no self-crossing between the predecessor and the actual configuration still holds.)

In conclusion we have shown, by producing counterexamples and explaining the underlying causes, that formulas (4) and (6) cannot be used to compute the writhe and the link of supercoiled DNA configurations encountered in magnetic tweezer experiments.

ACKNOWLEDGMENT

APPENDIX A: FULLER'S FORMULA IN A DETAILED EXAMPLE

In this appendix we compare, for a given example curve, the value computed from the double integral Wr^{CW} to the value computed from the single integral Wr^F. We start by introducing the parametrization of a circularly closed supercoiled plasmid (see Fig. 5). The parametrization is divided in four parts, called A, B, C, and D. Part A is a right-handed helix of radius unity, total arclength L_A, and helical angle θ_A (with $0 \le \theta_A < \pi/2$),

$$r_A = \begin{pmatrix} \sin \psi_A(s_A) \\ -\cos \psi_A(s_A) \\ s_A \cos \theta_A \end{pmatrix} \quad \text{and} \quad t_A = \frac{dr_A}{ds_A} = \begin{pmatrix} \sin \theta_A \cos \psi_A(s_A) \\ \sin \theta_A \sin \psi_A(s_A) \\ \cos \theta_A \end{pmatrix}$$

(A1)

with $s_A \in [0, L_A]$ and $\psi_A(s_A) = s_A \sin \theta_A$. We note

$$\stackrel{\text{def}}{\Delta \psi_A} = L_A \sin \theta_A.$$

We have $|t_A(s_A)| = 1$ for all s_A, and consequently s_A is the arclength in part A. The end loop B connects the two helices A and C,

$$r_B = \begin{pmatrix} \sin \Delta\psi_A \cos s_B + \cos \Delta\psi_A \sin \theta_A \sin s_B \cos s_B \\ -\cos \Delta\psi_A \cos s_B + \sin \Delta\psi_A \sin \theta_A \sin s_B \cos s_B \\ L_A \cos \theta_A + [\sin \theta_A - \sin \theta_B(s_B)]/(1 + 2\theta_A/\pi) \end{pmatrix}$$

$$\text{and} \quad t_B = \frac{dr_B}{ds_B}$$

(A2)

with $s_B \in [0, \pi]$, and $\theta_B(s_B) = \theta_A - s_B(1 + 2\theta_A/\pi)$. For this part B, $|t_B(s_B)| \neq 1$. Part C is a right-handed helix of radius unity, total arclength $L_C = L_A$, and helical angle $\theta_C = -\pi - \theta_A = \pi - \theta_A \mod 2\pi$,

$$r_C = \begin{pmatrix} -\sin \psi_C(s_C) \\ \cos \psi_C(s_C) \\ L_A \cos \theta_A + s_C \cos \theta_C \end{pmatrix} \quad \text{and}$$

$$t_C = \frac{dr_C}{ds_C} = \begin{pmatrix} \sin \theta_C \cos \psi_C(s_C) \\ \sin \theta_C \sin \psi_C(s_C) \\ \cos \theta_C \end{pmatrix}$$

(A3)

with $s_C \in [0, L_C]$ and $\psi_C(s_C) = \Delta\psi_A - s_C \sin \theta_C$. We have $|t_C(s_C)| = 1$ for all s_C, and consequently s_C is the arclength in part C. The end loop D closes the curve

$$r_D = \begin{pmatrix} \sin \theta_A \sin s_D \cos s_D \\ \cos s_D \\ [\sin \theta_D(s_D) - \sin \theta_A]/(1 + 2\theta_A/\pi) \end{pmatrix} \quad \text{and} \quad t_D = \frac{dr_D}{ds_D}$$

(A4)

with $s_D \in [0, \pi]$, and $\theta_D(s_D) = -\pi - \theta_A + s_D(1 + 2\theta_A/\pi)$. For this part D, $|t_D(s_D)| \neq 1$. We call Γ the union of the four parts: $\Gamma = \Gamma_A \cup \Gamma_B \cup \Gamma_C \cup \Gamma_D$. The curve has continuous derivatives, and finite jumps in its curvature.

1. Analytical calculation

The evaluation of the double integral of Eq. (2) in the limit $L_A \gg 1$ yields [46,11,37]

$$Wr^{CW}(\Gamma) \xrightarrow{L_A \to \infty} -\frac{L_A}{\pi} \sin \theta_A \cos \theta_A.$$

(A5)

The minus sign is due to the fact that the helices A and C are right handed.

We then compute $Wr^F(\Gamma, \Gamma_0)$, given by Eq. (3), using the reference curve Γ_0 of Fig. 6, top. The continuous deformation between Γ_0 and Γ is then parametrized by $\theta_{A_\lambda} \in [0, \theta_A]$. The reference curve of Fig. 6 (top) comes to mind naturally and makes calculations easiest, but yields antipodal events and hence an incorrect result, as we shall see now. The writhe of the reference curve Γ_0 is zero. Consequently we only must compute the integral $Fu(\Gamma, \Gamma_0)$ of Eq. (3) over the four different parts A, B, C, and D. Clearly when the plasmid
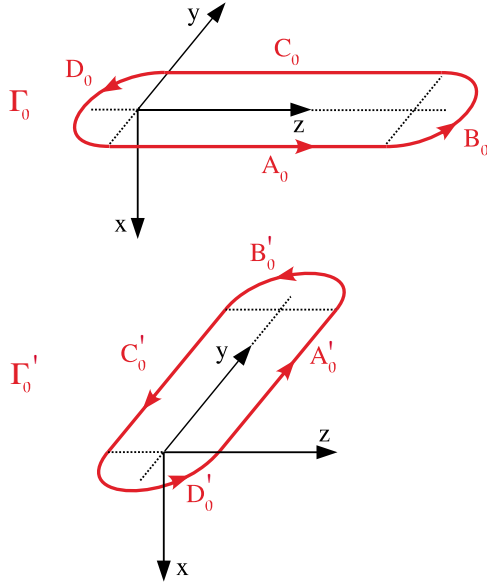
FIG. 6. (Color online) Two reference curves used to compute Wr^F for the supercoiled plasmid of Fig. 5.

is long enough, i.e., when L_A is large, the contribution to $Fu(\Gamma,\Gamma_0)$ of the helical parts A and C becomes dominant. Indeed their contribution scales with L_A while the contribution of the end loops B and D remains bounded. Consequently we focus on the contributions of the helical parts A and C, for large values of L_A, that is we look at the limit $Fu(\Gamma,\Gamma_0) \to Fu_A(\Gamma,\Gamma_0) + Fu_C(\Gamma,\Gamma_0)$ when $L_A \to \infty$ [47]. For the helical part A, the corresponding tangent of the reference curve is $t_{A_0} = (0,0,1)$. Fuller integral for part A is then

$$Fu_A = \int_0^{L_A} \frac{d\psi_A}{ds_A}(1 - \cos\theta_A)ds_A = \sin\theta_A(1 - \cos\theta_A)L_A.$$

(A6)

For the helical part C, the corresponding tangent of the reference curve is $t_{C_0} = (0,0,-1)$. The Fuller integral for part C is then

$$Fu_C = \int_0^{L_C} -\frac{d\psi_C}{ds_C}(1 + \cos\theta_C)ds_C$$

$$= \sin\theta_C(1 + \cos\theta_C)L_C = Fu_A.$$

(A7)

Neglecting the end loop contributions we arrive at

$$Wr^F(\Gamma,\Gamma_0) = Wr(\Gamma_0) + \frac{1}{2\pi}Fu(\Gamma,\Gamma_0)$$

(A8)

$$= \frac{1}{2\pi}(Fu_A + Fu_B + Fu_C + Fu_D)$$

(A9)

$$\simeq \frac{1}{2\pi}(Fu_A + Fu_C) = \frac{L_A}{\pi}\sin\theta_A(1 - \cos\theta_A).$$

(A10)

We first remark that $Wr^F(\Gamma,\Gamma_0) > 0$ although $Wr^{CW}(\Gamma) < 0$ [see Eq. (A5)]. The discrepancy $Wr^F(\Gamma) \neq Wr^{CW}(\Gamma)$ is due to the fact that in the continuous deformation $\theta_{A_\lambda} \in [0, \theta_A]$ from

the curve Γ_0 of Fig. 6 top to the plasmid of Fig. 5, there are antipodal events. These events happen each time the middle point of the end loop B is pointing towards $-\mathbf{e_y}$ and hence becomes antipodal to the corresponding tangent in B_0. As θ_{A_λ} is increased, such an event happens once each time

$$\Delta\psi_{A_\lambda} \overset{\text{def}}{=} L_A \sin\theta_{A_\lambda}$$

increases by an amount of 2π. In the entire deformation there will be $\Delta\psi_A/(2\pi)$ antipodal events. Each event introduces a shift between $Wr^{CW}(\Gamma)$ and $Wr^F(\Gamma,\Gamma_0)$ of 2, the difference $Wr^F(\Gamma,\Gamma_0) - Wr^{CW}(\Gamma)$ should then be equal to $2\Delta\psi_A/(2\pi) = (L_A/\pi)\sin\theta_A$, which can be verified by comparing Eq. (A5) and (A10). A natural way to try to avoid the presence of these antipodal points is to rotate the reference curve, e.g., choose Γ_0' of Fig. 6 bottom as reference curve. In this case $Fu_A = -\cos\theta_A\sin\theta_A\int_0^{\Delta\psi_A}\sin\psi/(1 + \sin\theta_A\sin\psi)d\psi$ and $Fu_C = \cos\theta_A\sin\theta_A\int_0^{\Delta\psi_A}\sin\psi/(1 - \sin\theta_A\sin\psi)d\psi \neq Fu_A$. Here again the sum $Fu_A + Fu_C$ dominates $Fu(\Gamma,\Gamma_0')$. Integration shows that $Fu_A + Fu_C = 2L_A\sin\theta_A(1 - \cos\theta_A) + \eta(L_A,\theta_A)$, with $|\eta(L_A,\theta_A)| \leq 1 - \cos\theta_A$, which is not the correct result. Antipodal events are in fact still present with this rotated reference curve Γ_0' and trying another rotation will not help, as explained in Appendix B.

2. Numerical verification

In Fig. 5, a right-handed circularly closed plasmid is drawn with $\theta_A = \pi/6$, $L_A = 5\pi$. The viewpoint selected to draw the curve in Fig. 5 is such that three (negative) crossings appear. For some other viewpoints, only two crossings appear. The writhe being the average number of signed crossings one sees from all possible viewpoints, it is relatively easy to convince oneself that its value for the curve of Fig. 5 lies in between -2 and -3. A numeric discretization scheme [44] of the double integral of Eq. (2) with 600 points yields $Wr^{CW}(\Gamma) \simeq -2.2049$. A numerical integration of $Fu(\Gamma,\Gamma_0) = Fu_A + Fu_B + Fu_C + Fu_D$ yields $Wr^F(\Gamma,\Gamma_0)[=Wr^F(\Gamma,\Gamma_0')] \simeq -0.2050$. The difference between $Wr^{CW}(\Gamma)$ and $Wr^F(\Gamma,\Gamma_0)$ is -2, which indicates that the net number of signed antipodal events is -1, as shown in Appendix B.

APPENDIX B: CLOSED CIRCUIT THEOREM

1. Antipodal points and self-crossings

In Fig. 7 we show a family of curves along a continuous deformation. The deformation starts and ends with the same curve: We have a closed circuit. The "stadium" shaped curve $\Gamma_{\lambda=0}$ is continuously deformed through curves Γ_λ, as λ increases from $\lambda=0$ to $\lambda=1$, to the supercoiled plasmid Γ_1. The plasmid is then deformed back to the "stadium" shaped curve, through another path, as λ increases from $\lambda=1$ to $\lambda=2$. The values $\lambda=0$ and $\lambda=2$ refer to the same curve, the reference curve, which plays a special role. This reference curve is chosen to be fairly simple, in particular $Wr(\Gamma_0)=0$. All the curves in the continuous deformation share a parametrization with parameter s (not necessarily the arclength)
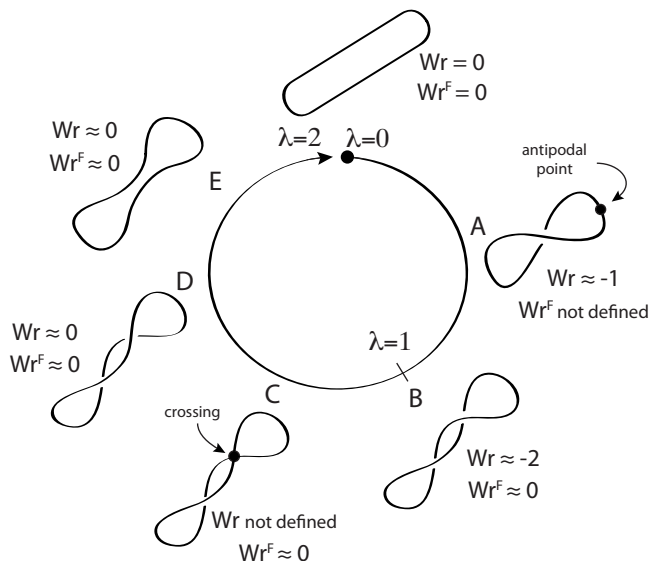
FIG. 7. A closed circuit with one antipodal point and one self-crossing.

taking values from $s=0$ to $s=L$. We recall that an antipodal point is a point on a curve Γ_λ such that the tangent $t_\lambda(s^\star)$ to Γ_λ at $s=s^\star$ is aligned and in opposite direction with the tangent $t_0(s^\star)$ to the reference curve Γ_0, i.e., an antipodal point is such that $t_\lambda(s^\star)\cdot t_0(s^\star)=-1$. An antipodal point is always defined with regard to a certain reference curve. Along a continuous deformation there may be λ values where the curves Γ_λ have antipodal points to Γ_0, and there may be λ values where the curves Γ_λ self-intersect. The closed circuit theorem claims that in any closed circuit the (signed) number of self-intersections is equal to the (signed) number of antipodal points. For example, in the closed circuit of Fig. 7 there is one antipodal point and one self-crossing. This theorem was proposed and proven in [43] for a particular case of reference curve, a straight line. Here we give an outline of a proof which is valid for more general reference curves: Formula (2) has a ± 2 discontinuity at each self-crossing event encountered in the closed circuit, but no discontinuity during antipodal events. On the contrary formula (3) has no discontinuity during self-crossing events but a ± 2 discontinuity at each antipodal event [13]. Formula (2) and (3) by definition agree when applied to the reference curve, and furthermore they may only differ by an even integer: $Wr^{CW}=Wr^F$ mod 2. If we now follow the closed circuit, each formula will have its own discontinuities but both must eventually agree again at the end of the circuit. It follows that the number of discontinuities (respectively, events) of one kind must be equal to the number of discontinuities (respectively, events) of the other kind.

2. No parallel between $Wr^{CW}(\Gamma)$ and $Wr^F(\Gamma, \Gamma_0)$

The quantity $Wr^{CW}(\Gamma)$ is not defined on curves that are self-intersecting, e.g., curve C in Fig. 7. The quantity $Wr^F(\Gamma, \Gamma_0)$ is not defined on curves Γ that have an antipodal point to Γ_0, e.g., curve A in Fig. 7. These two properties, once considered with the fact that in any closed circuit the

number of configurations with self-crossing is equal to the number of configurations with antipodal points, could lead one to believe that some parallel exists between $Wr^{CW}(\Gamma)$ and $Wr^F(\Gamma, \Gamma_0)$. In fact in [43] it is proposed that, in the computation of the mean writhe (or link) of a statistical ensemble of curves, avoiding self-crossings was equivalent to avoiding antipodal points. Moreover, it was inferred that for such statistical ensemble of curves, Fuller's formula, Eq. (3), could be used safely provided that curves with antipodal point(s) were discarded when generating the statistical ensemble. We argue that this is not the case as Fuller's formula does not yield the right result for the (many) curves that have no antipodal point: For example, curve B in Fig. 7. Again, Fuller's formula can only be used for a curve Γ_λ^- if one can devise a continuous deformation from Γ_λ^- to Γ_0 where none of the curves Γ_λ with $0 < \lambda \le \bar{\lambda}$ has antipodal points. For curve B in Fig. 7 this is not the case since the curve A has an antipodal point. Accordingly Fuller's formula does not yield the correct value for the writhe of curve B, as explicitly computed in Appendix A. In conclusion we stress that there is no parallel between the two formulas $Wr^{CW}(\Gamma)$ and $Wr^F(\Gamma, \Gamma_0)$: On the one hand $Wr^{CW}(\Gamma)$ yields the correct value of the writhe of a curve as soon as the curve does not self-intersect and on the other hand $Wr^F(\Gamma, \Gamma_0)$ often yields an incorrect value for the writhe of a curve even if this curve has no antipodal point.

All that is exposed here for the curves in Fig. 7 is directly applicable to the configurations of Fig. 2 and shows that the writhe (respectively, the link) of the configurations with $Z < Z_B$ in Fig. 4 is not given by Eq. (3) [respectively, Eq. (6)].

3. Impossibility to use the "stadium" shaped curve as reference curve

Fuller's theorem [12] states that as soon as there is a continuous deformation between Γ and Γ_0 which is free of antipodal points and self-crossings (we called "good" such a deformation), $Wr^F(\Gamma, \Gamma_0)$ yields the correct value for the writhe of the closed curve Γ. In Fig. 7 the deformation from $\lambda=0$ to $\lambda=1$ is a "bad" deformation as it contains one antipodal event. We then conclude that $Wr^F(\Gamma_1, \Gamma_0)$ yields an incorrect value. But one might say that another deformation between Γ_1 and Γ_0, with neither self-crossing nor antipodal event, could exist. We show here that this is not the case. *Statement*: No "good" deformation between Γ_1 and Γ_0 of Fig. 7 exists.

Proof: Assume a "good" deformation exists. Then we can build a closed circuit by joining this proposed deformation and the (reversed) actual deformation $\lambda \in [0,1]$ in Fig. 7. One would then have a closed circuit with one antipodal point and no self-crossing, in contradiction with the result established in [43]. Hence no such "good" deformation exists. ∎

This means that as soon as one "bad" deformation exists between a reference curve Γ_0 and a curve Γ the formula $Wr^F(\Gamma, \Gamma_0)$ does not yield the correct result and no "good" deformation can exist. A consequence of this

is that rotating the reference curve of Appendix A (Fig. 6, top) to introduce a new, and "good," reference curve (e.g., Fig. 6, bottom) is hopeless. To show this we first introduce a "bad" deformation between the rotated reference curve (e.g., Fig. 6, bottom) and the supercoiled plasmid of Fig. 5: We untangle the plasmid using a self-crossing, as in *C* of Fig. 7, to obtain a "stadium" shaped curve which we subsequently rotate to the (rotated) reference curve. The existence of this "bad" deformation means that no "good" deformation can exist.

[1] S. B. Smith, L. Finzi, and C. Bustamante, Science **258**, 1122 (1992).
[2] T. R. Strick, J.-F. Allemand, D. Bensimon, A. Bensimon, and V. Croquette, Science **271**, 1835 (1996).
[3] Christopher Deufel, Scott Forth, Chad R. Simmons, Siavash Dejgosha, and Michelle D. Wang, Nat. Methods **4**, 223 (2007).
[4] Thijn van der Heijden, John van Noort, Hendrikje van Leest, Roland Kanaar, Claire Wyman, Nynke Dekker, and Cees Dekker, Nucleic Acids Res. **33**, 2099 (2005).
[5] Andrey Revyakin, Richard H. Ebright, and Terence R. Strick, Proc. Natl. Acad. Sci. U.S.A. **101**, 4776 (2004).
[6] G. Călugăreanu, Rev. Math. Pures Appl. **4**, 5 (1959).
[7] G. Călugăreanu, Czech. Math. J. **11**, 588 (1961).
[8] J. White, Am. J. Math. **91**, 693 (1969).
[9] M. R. Dennis and J. H. Hannay, Proc. R. Soc. London, Ser. A **461**, 3245 (2005).
[10] F. Brock Fuller, Proc. Natl. Acad. Sci. U.S.A. **68**, 815 (1971).
[11] E. L. Starostin, e-print arXiv:physics/0212095.
[12] F. Brock Fuller, Proc. Natl. Acad. Sci. U.S.A. **75**, 3557 (1978).
[13] Jürgen Aldinger, Isaac Klapper, and Michael Tabor, J. Knot Theory Ramif. **4**, 343 (1995).
[14] V. Rossetto and A. C. Maggs, J. Chem. Phys. **118**, 9864 (2003).
[15] V. Rossetto, Europhys. Lett. **69**, 142 (2005).
[16] Gert van der Heijden, Mark A. Peletier, and Robert Planqué, Q. Appl. Math. **65**, 385 (2007).
[17] B. Fain, J. Rudnick, and S. Östland, Phys. Rev. E **55**, 7364 (1997).
[18] B. Fain and J. Rudnick, Phys. Rev. E **60**, 7239 (1999).
[19] J. David Moroz and Philip Nelson, Proc. Natl. Acad. Sci. U.S.A. **94**, 14418 (1997).
[20] C. Bouchiat and M. Mézard, Phys. Rev. Lett. **80**, 1556 (1998).
[21] C. Bouchiat and M. Mézard, Eur. Phys. J. E **2**, 377 (2000).
[22] J. David Moroz and Philip Nelson, Macromolecules **31**, 6333 (1998).
[23] Philip Nelson, Biophys. J. **74**, 2501 (1998).
[24] J. F. Marko, Phys. Rev. E **57**, 2134 (1998).
[25] J. F. Marko, Phys. Rev. E **59**, 900 (1999).
[26] Haijun Zhou, Yang Zhang, and Zhong-can Ou-Yang, Phys. Rev. E **62**, 1045 (2000).
[27] Pik-Yin Lai and Zicong Zhou, J. Chem. Phys. **118**, 11189 (2003).
[28] D. Garrivier and B. Fourcade, Europhys. Lett. **49**, 390 (2000).
[29] Zicong Zhou and Pik-Yin Lai, Physica A **350**, 70 (2005).
[30] Zhou Haijun, Zhang Yang, and Ou-Yang Zhong-can, Phys. Rev. Lett. **82**, 4560 (1999).
[31] R. Zandi and J. Rudnick, Phys. Rev. E **64**, 051918 (2001).
[32] Zicong Zhou and Pik-Yin Lai, Int. J. Mod. Phys. B **17**, 3021 (2003).
[33] Zicong Zhou, Mod. Phys. Lett. B **19**, 249 (2005).
[34] Supurna Sinha, Phys. Rev. E **70**, 011801 (2004).
[35] V. Rossetto and A. C. Maggs, Phys. Rev. Lett. **88**, 089801 (2002).
[36] O. Kratky and G. Porod, Recl. Trav. Chim. Pays-Bas **68**, 1106 (1949).
[37] E. L. Starostin, in *Physical and Numerical Models in Knot Theory Including Applications to the Life Sciences*, edited by J. A. Calvo, K. C. Millett, E. J. Rawdon, and A. Stasiak, Vol. 36 Series on Knots and Everything (World Scientific, Singapore, 2005), Chap. 26, pp. 525–545.
[38] E. L. Starostin, J. Phys. A **35**, 6183 (2002).
[39] S. Neukirch, Phys. Rev. Lett. **93**, 198107 (2004).
[40] T. R. Strick, J.-F. Allemand, D. Bensimon, and V. Croquette, Biophys. J. **74**, 2016 (1998).
[41] G. H. M. van der Heijden and J. M. T. Thompson, Nonlinear Dyn. **21**, 71 (2000).
[42] J. M. T. Thompson, Eur. Phys. J. E (to be published).
[43] Joseph Samuel, Supurna Sinha, and Abhijit Ghosh, J. Phys.: Condens. Matter **18**, S253 (2006).
[44] David Swigon, Bernard D. Coleman, and Irwin Tobias, Biophys. J. **74**, 2515 (1998).
[45] Jason Cantarella, SIAM (Soc. Ind. Appl. Math.) J. Numer. Anal. **42**, 1846 (2005).
[46] Sébastien Neukirch and Gert van der Heijden, J. Elast. **69**, 41 (2002).
[47] F. H. C. Crick, Proc. Natl. Acad. Sci. U.S.A. **73**, 2639 (1976).